Monitoring the Hydrophobic Interactions of Internally Pyrene-Labeled Poly(ethylene oxide)s in Water by Fluorescence Spectroscopy

Sam Lee

R & D Center, Dupont Canada, 461 Front Road, Kingston, ON, K7L 5A5 Canada

Jean Duhamel*

Institute for Polymer Research, Department of Chemistry, University of Waterloo, Waterloo, ON, N2J 3G1 Canada

Received July 23, 1998; Revised Manuscript Received October 16, 1998

ABSTRACT: Steady-state and fluorescence decay measurements have been carried out on aqueous solutions of poly(ethylene glycol)s made of a central chain spanning two pyrene labels and flanked by overhangs of various lengths. These decays exhibit excimer formation kinetics which cannot be explained within the theoretical framework of the classic Birks' scheme. The decay analysis is complicated by the existence of hydrophobic associations between the pyrene groups. We have analyzed our time-resolved fluorescence decays by deriving a dynamic version of a model originally proposed by Char et al. (*Macromolecules* **1989**, *22*, 3177−3180) where the pyrene excimer is formed in a sequential manner. A diffusion process brings the two chromophores within a *capture* volume where the excimer is produced at a much higher rate. An analysis of our fluorescence decays based on this approach yields kinetic parameters which are consistent with the Char et al. model and earlier observations made on these systems. As the size of the overhang increases, the diffusion-controlled excimer formation rate decreases as was found previously in organic solvents, and the degree of association increases as well. The excimer formation process within the *capture* volume is very rapid. This quantitative analysis provides us with a detailed picture of these systems.

Introduction

Proteins and polynucleotides can spontaneously fold into well-defined structures which are stabilized by a variety of noncovalent forces that include hydrogen bonds, electrostatic forces, steric packing, and hydrophobic effects (referred to as the solvophobic effect when the solvent is not water).[1] Understanding how these forces affect the folding pathways of proteins and polynucleotides is the subject of active research.[2] Among these forces, solvophobic effects have also been shown to be important for the design of self-assembling synthetic polymer systems that mimic biological systems.[3] Furthermore, solvophobic forces are key players for the design of associating polymers having desired associating characteristics, a research area which has found many practical applications. Associating polymers are used as thickeners in paints, drag reducing agents in pipelines, colloid stabilizers in oil and paint, and oil recovery enhancers.[4] Being able to quantitatively characterize well-defined model compounds that display controlled contents of solvophobic and solvophilic material is an important step toward understanding the subtle balance taking place between solvophobic and solvophilic forces.

Monodisperse water-soluble polymers onto which hydrophobic chromophores have been covalently attached at specific positions constitute valuable model compounds for this purpose.[5] As a hydrophobic chromophore, pyrene is particularly attractive because it also allows the study of polymer chain dynamics, a process reminiscent of chain folding in the case of proteins and polynucleotides. Upon absorption of a photon, an excited pyrene can form an excimer via diffusional encounter with a ground-state pyrene. The rate of excimer formation yields information about the dynamics of the polymer chain to which the pyrene groups are attached.[6] To date, most studies on water-soluble associating polymers with a covalently bound chromophore have focused on polymers where the chromophores are attached either randomly along the polymer backbone or selectively at the chain ends.[7] Recently, a series of poly(ethylene glycol)s (PEGs) has been synthesized with a central chain spanning two pyrene labels and flanked by end chains of different lengths.[8,9] With these polymers, one can evaluate the effect of molecular weight of the overhang on the rate of internal cyclization as well as the hydrophobic interactions between the two insoluble chromophores. The internal cyclization of these polymers in organic solvents has been the object of a first study.[9] In organic solvents, the fluorescence decays of the monomer and the excimer follow the classic Birks' scheme[10] where the excimer decay is biexponential and the monomer decay is also a biexponential function to which a third exponential has been added to account for unquenched pyrene monomer. In water, however, the fluorescence decays of the monomer and the excimer are clearly not biexponential,[9] and even when the presence of unquenched monomer is accounted for, these fluorescence decays cannot be analyzed with the classic Birks' scheme.

Complicated decays have been observed in numerous studies involving water-soluble polymers labeled with pyrene.[7] Although an excimer does not exist in the ground state, hydrophobic interactions induce the formation of ground-state pyrene dimers where two pyrene monomers are held in close contact. Upon excitation, these pyrene pairs form an excimer with little or no

* To whom correspondence should be addressed.

10.1021/ma981160m CCC: $15.00
Published on Web 12/04/1998

Scheme 1

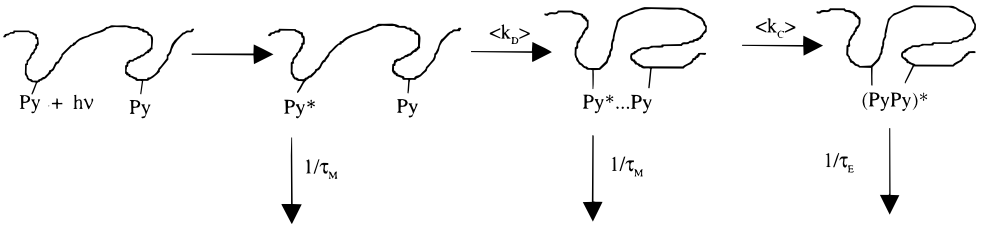

delay due to their short distance of separation and the excimer decay exhibits a short or no rise-time. The pyrene ground-state dimers are supposedly the cause for the complicated behavior of the monomer and excimer fluorescence decays, making the kinetic analysis rather complex. In addition to these intramolecular hydrophobic interactions between pyrene groups, intermolecular associations can also be present if the molecule contains too much hydrophobic material. Often qualitative information is retrieved from a multiexponential fit of the pyrene monomer fluorescence decay by calculating the average decay time of the pyrene chromophore. A shorter average lifetime implies a more efficient quenching of the dye, which can then be related to the structure of the polymer under study. However, such basic analysis does not provide quantitative information about the effect of overhang length on the fraction of associated hydrophobic moieties and the folding dynamics of the polymer chain. This is important information as it provides the means of tailoring an associating polymer (AP) with the proper {hydrophobic content}/{overhang length} balance, resulting in the targeted associating strength. Only quantitative analysis of the fluorescence decays combined with steady-state fluorescence measurements can provide such a detailed picture of these systems.

We set out to obtain quantitative information about the intramolecular hydrophobic associations occurring between the pyrene groups of these polymers. Steady-state fluorescence measurements were carried out to establish whether the polymers associate either intra- or intermolecularly in the concentration range investigated (0.1 μM < [Poly] < 2.0 μM). All fluorescence decays were obtained with polymer concentrations between 1.1 and 1.3 μM. The analysis of the fluorescence decays is based on a model that was originally proposed by Char et al. as a way to rationalize the steady-state fluorescence measurements of a pyrene end-capped PEG.[11] In their model, the excimer is formed via a *capture* process of the hydrophobic chromophores. The *capture* radius is defined as follows for pyrene groups located at the ends of the polymer chain. "If one pyrene end is within a distance of twice the *capture* radius from the other, the two are attracted to each other yielding an excimer emission." For a monodisperse pyrene end-capped PEG of M_w 4800, Char et al. found the *capture* radius R_c to equal 20 Å. The kinetic implications of a *capture* volume are that pyrene excimers are produced via at least two sequential processes. First, the pyrene chromophores will come within a distance $2R_C$ of each other via diffusion which will occur with a rate constant $\langle k_D \rangle$. When inside the sphere of radius R_C, the chromophores will form an excimer with a rate constant $\langle k_C \rangle$. Within the *capture* volume, the excimer can dissociate with a dissociation rate constant k_{-C}. A chromophore will escape the *capture* volume and diffuse away with a rate constant k_{-D}. These kinetic pathways are depicted in Scheme 1, where k_{-C} and k_{-D} have been set to equal 0 s^{-1}. τ_M and τ_E are the lifetimes of the monomer and the excimer, respectively. The brackets indicate that the pyrene local concentration is accounted for in the rate constant.

Table 1. Chemical Structure of the Pyrene-Labeled PEGs Used in This Study Using (EO) for an Ethylene Oxide Unit (CH_2CH_2O) and Py for Pyrene

Compound	Chemical structure
EO_{47}-Py-EO_{87}-Py-EO_{47}	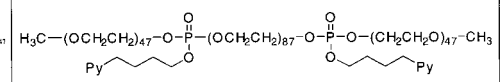
EO_{17}-Py-EO_{87}-Py-EO_{17}	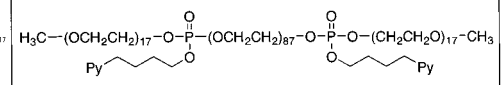
EO_{12}-Py-EO_{87}-Py-EO_{12}	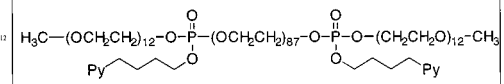
EO_{02}-Py-EO_{87}-Py-EO_{02}	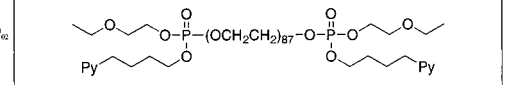
Py-EO_{87}-Py	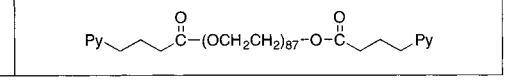

To the best of our knowledge, this is the first time that a quantitative analysis of the fluorescence decays of pyrene-labeled PEGs has been reported, which reveals kinetic and structural details of these self-assembling molecules.

Experimental Section

Sample Synthesis and Preparation. Spectroscopic grade tetrahydrofuran (THF) was purchased from Caledon Laboratories and used as received. Distilled water was treated with a Millipore Milli-Q water system. The synthesis and characterization of all the compounds listed in Table 1 has been reported elsewhere.[8] The poly(ethylene glycol) used to construct the central chain in all these polymers had a molecular weight of $M_n = 3841$, which corresponds to a number average of 87 oxyethylene monomer units. $PyEO_{87}Py$ was made by direct acid-catalyzed esterification of the hydroxyl ends of this poly(ethylene glycol) with 4-(1-pyrenyl)-butyric acid.[12] The other four labeled polymers were obtained by coupling the appropriate 4-(1-pyrenyl)butyl oligooxyethylene *N*,*N*-diisopropylphosphoramidite to the hydroxyl ends of the poly(ethylene glycol) 3841 followed by oxidative workup.[12]

To ensure that no free label was present in the solution, each polymer sample was purified by repeated precipitations in THF using diethyl ether. This was followed with gel permeation chromatography by running THF solutions of the

polymers through a Waters gel permeation chromatograph fitted with a Jordi gel DVB mixed bed column and UV and DRI detectors. The main peak was collected and the polymer concentration of the solution was estimated by UV−vis absorption measurements. Water solutions of these polymers were prepared by evaporating carefully weighed aliquots of THF solution under a gentle flow of nitrogen and dissolving the dry polymer into a known amount of deionized distilled water. Dilute solutions of these purified polymers (0.1 μM < [Poly] < 2.0 μM) were prepared in 1 cm quartz cells and degassed with nitrogen prior fluorescence measurements.

Kinetic Analysis. Rheological studies performed on PEGs carrying hydrophobic moieties have shown that the hydrophobic associations are stable on the msec time scale.[13] It is thus reasonable to assume that little escape of the hydrophobic chromophores from the *capture* volume occurs during the time pyrene remains excited. Furthermore the dissociation rate of the pyrene excimer is usually small, leading to Scheme 1 where k_{-D} and k_{-C} were set to equal 0 s^{-1}.

Three differential equations are enough to describe this system:

$$\frac{d[M_D^*]}{dt} = -\left(\langle k_D\rangle + \frac{1}{\tau_M}\right)[M_D^*] \quad (1)$$

$$\frac{d[M_C^*]}{dt} = \langle k_D\rangle[M_D^*] - \left(\langle k_C\rangle + \frac{1}{\tau_M}\right)[M_C^*] \quad (2)$$

$$\frac{d[E^*]}{dt} = \langle k_C\rangle[M_C^*] - \frac{1}{\tau_E}[E^*] \quad (3)$$

Here M_D^* characterizes the excited pyrene undergoing diffusion, M_C^* represents the excited pyrene trapped in the *capture* volume, and E* is the pyrene excimer.

According to Scheme 1, the monomer and the excimer decays are fitted by biexponential and triexponential functions, respectively. Scheme 1 is further complicated because each polymer has a small fraction of its chains labeled with a ketopyrene group. The ketopyrene group prevents excimer formation so that the polymer chains containing this group emit with the unquenched lifetime of pyrene τ_M.[8] Consequently, a third exponential must be introduced in the monomer decay to account for pyrene groups that are unable to form excimers. Equations 4 and 5 describe the resulting

$$[M^*] = \left([M_C^*]_0 + \frac{\langle k_D\rangle[M_D^*]_0}{\langle k_D\rangle - \langle k_C\rangle}\right)e^{-(\langle k_C\rangle + 1/\tau_M)t} + \frac{\langle k_C\rangle[M_D^*]_0}{\langle k_C\rangle - \langle k_D\rangle}e^{-(\langle k_D\rangle + 1/\tau_M)t} + [M_U^*]_0\, e^{-(t/\tau_M)} \quad (4)$$

$$[E^*] = -\frac{\langle k_C\rangle}{\langle k_C\rangle + \frac{1}{\tau_M} - \frac{1}{\tau_E}}\left([M_C^*]_0 + \frac{\langle k_D\rangle\,[M_D^*]_0}{\langle k_D\rangle - \langle k_C\rangle}\right)e^{-(\langle k_C\rangle + 1/\tau_M)t} + \frac{\langle k_D\rangle}{\langle k_D\rangle + \frac{1}{\tau_M} - \frac{1}{\tau_E}}\frac{\langle k_C\rangle[M_D^*]_0}{\langle k_D\rangle - \langle k_C\rangle}e^{-(\langle k_D\rangle + 1/\tau_M)t} + \left([E^*]_0 + \frac{\langle k_C\rangle[M_C^*]_0}{\langle k_C\rangle + \frac{1}{\tau_M} - \frac{1}{\tau_E}} + \frac{\langle k_D\rangle\langle k_C\rangle[M_D^*]_0}{\left(\langle k_D\rangle + \frac{1}{\tau_M} - \frac{1}{\tau_E}\right)\left(\langle k_C\rangle + \frac{1}{\tau_M} - \frac{1}{\tau_E}\right)}\right)e^{-(t/\tau_E)} \quad (5)$$

monomer and excimer decays, where $[M_U^*]_0$ represents the contribution from unquenched pyrene monomer. $\langle k_C\rangle$ is the rate of excimer formation within the *capture* volume. According to the Char et al. model,[11] this excimer formation process occurs on a fast time scale so that the following sequence should be observed:

$$\tau_1\left\{ = \left(\langle k_C\rangle + \frac{1}{\tau_M}\right)^{-1}\right\} << \tau_2\left\{ = \left(\langle k_D\rangle + \frac{1}{\tau_M}\right)^{-1}\right\} < \tau_M \quad (6)$$

Since τ_M is the decay time of unquenched pyrene, it constitutes the longest possible relaxation time in the monomer decay. Values of τ_E have been reported to range from 43.5 ns in acetone up to 65 ns in cyclohexane.[10]

Time-Resolved Fluorescence Measurements. Decay curves were obtained by the time-correlated single photon counting technique. These were measured by a Photochemical Research Associates Inc. System 2000. The excitation wavelength was 345 nm and the fluorescence from the pyrene monomer and excimer were monitored at 376 and 510 nm, respectively. To block potential light scattering leaking through the detection system, filters were used with a cutoff at 370 and 495 nm to acquire the fluorescence decays of the pyrene monomer and excimer, respectively. For $EO_{47}PyEO_{87}PyEO_{47}$ in water, the monomer and excimer decays were collected over 512 and 256 channels, respectively. For the other polymers, both monomer and excimer decays were collected over 512 channels. A total of 20 000 counts was collected at the peak maximum of the lamp and the decay curves. The analysis of the decay curves were performed with the δ-pulse deconvolution.[14] Reference decay curves of degassed solutions of PPO [2,5-diphenyloxazole] in cyclohexane (τ = 1.42 ns) and BBOT [2,5-bis(5-*tert*-butyl-2-benzoxazolyl)thiophene] in ethanol (τ = 1.47 ns) were used for the analysis of the monomer and excimer decay curves, respectively.

Fitting Procedure. Due to the complexity arising from fitting accurately a decay with a sum of exponentials (in this case three exponentials for the monomer and the excimer), the fluorescence decays were fitted using a global analysis approach.[15] The monomer and excimer decays obtained from a same polymer sample were fitted simultaneously according to eqs 7 and 8. The lifetimes τ_1 and τ_2 were forced to be equal in

$$[M^*] = A_{M1}\exp\left(-\frac{t}{\tau_1}\right) + A_{M2}\exp\left(-\frac{t}{\tau_2}\right) + A_{M3}\exp\left(-\frac{t}{\tau_M}\right) \quad (7)$$

$$[E^*] = A_{E1}\exp\left(-\frac{t}{\tau_1}\right) + A_{E2}\exp\left(-\frac{t}{\tau_2}\right) + A_{E3}\exp\left(-\frac{t}{\tau_E}\right) \quad (8)$$

the monomer and excimer decays. The lifetime τ_M is fixed in the analysis to be equal to that of the longest pyrene monomer decay which was found to be 170 ns. The parameters were optimized with the Marquardt−Levenberg algorithm.[16] The goodness of the fits was judged from the global reduced χ_g^2, and the residuals and the autocorrelation of the residuals. $\langle k_D\rangle$ and $\langle k_C\rangle$ are retrieved from τ_1 and τ_2. The fractions of pyrene undergoing diffusion $f_{[M_D^*]_0}$, excited pyrene trapped in the *capture* volume $f_{[M_C^*]_0}$, and ground-state pyrene dimers $f_{[E^*]_0}$ are determined from the preexponential factors a_{Mi} and a_{Ei} (with i = 1, 2, 3) according to eqs 4−6. Error bars for the parameters obtained from analysis of the fluorescence decays were obtained by simulating 20 fluorescence decays with different Poisson noise patterns, fitting the simulated decays, and calculating the standard deviations of the retrieved parameters.[17]

Steady-State Fluorescence Measurements. Fluorescence spectra were obtained with a right angle configuration on a Photon Technology International LS-100 steady-state system with a pulsed xenon flash lamp as the light source. The samples were excited at 345 nm. The fluorescence intensities of the monomer (I_M) and of the excimer (I_E) were calculated by taking the integrals under the fluorescence spectra from 373 up to 379 nm for the pyrene monomer, and from 500 up to 530 nm for the pyrene excimer. Each fluorescence spectra was recorded four times, and the average of these measurements is shown. Error bars were smaller than the symbols used in Figure 2.

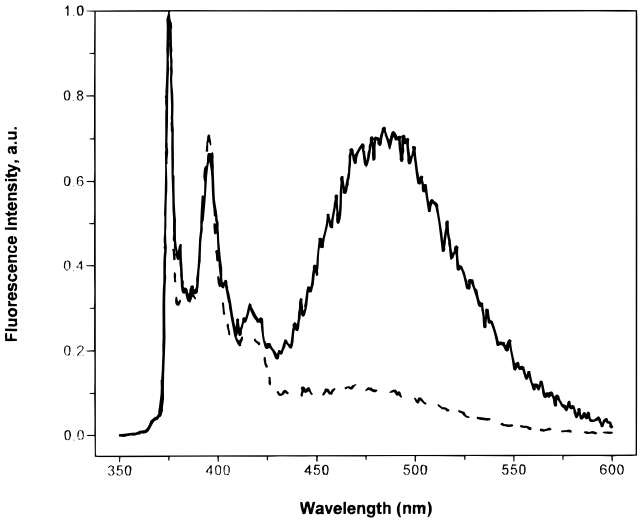

Figure 1. Fluorescence spectra of Py−EO_{87}−Py in THF (- - -, [Poly] = 0.86 μM, low excimer fluorescence intensity) and water (—, [Poly] = 0.91 μM, large excimer fluorescence intensity) normalized at the 0−0 peak (λ_{0-0} = 375 nm). The noise in the data was a consequence of the low chromophore concentrations used in these measurements.

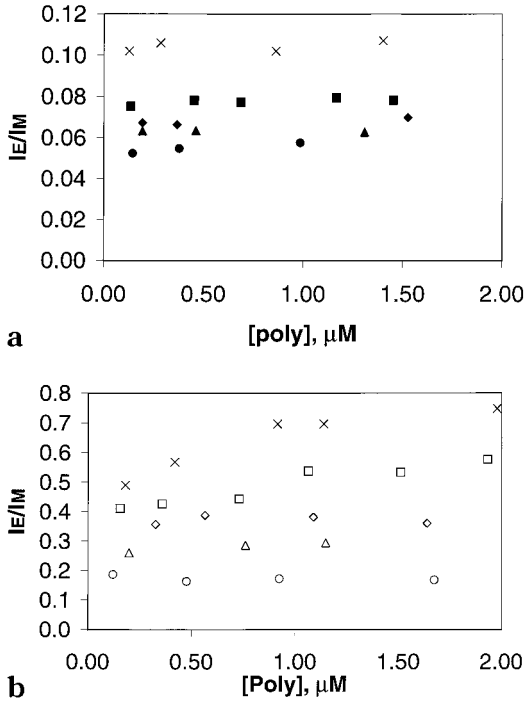

Figure 2. Ratios I_E/I_M as a function of polymer concentration in (a) THF (×, Py−EO_{87}−Py; ■, EO_{02}−Py−EO_{87}−Py−EO_{02}; ◆, EO_{15}−Py−EO_{87}−Py−EO_{15}; ▲, EO_{17}−Py−EO_{87}−Py−EO_{17}; ●, EO_{47}−Py−EO_{87}−Py−EO_{47}), and (b) water (×, Py−EO_{87}−Py; □, EO_{02}−Py−EO_{87}−Py−EO_{02}; ◇, EO_{15}−Py−EO_{87}−Py−EO_{15}; △, EO_{17}−Py−EO_{87}−Py−EO_{17}; ○, EO_{47}−Py−EO_{87}−Py−EO_{47}). λ_{ex} = 345 nm.

Results

An associating polymer (AP) is usually composed of a soluble backbone onto which insoluble moieties have been attached. A backbone specific solvent will induce associations of the insoluble moieties, which disappear when the AP is dissolved in an aspecific solvent. This is illustrated in Figure 1 where the fluorescence spectra of Py−EO_{87}−Py are presented in THF and deionized distilled water. Hydrophobic associations in water induce enhanced formation of pyrene excimer when compared with a solution of the same polymer in THF, an aspecific solvent. These hydrophobic associations induce the formation of a ground-state pyrene excimer which distorts the excitation spectra and complicates the fluorescence decays, which analysis requires more parameters than the classic Birks' type.[9]

Steady-state fluorescence measurements were carried out with polymer solutions in THF and distilled deionized water (dH_2O) in order to investigate the processes of excimer formation. The ratio of the excimer fluorescence intensity I_E over that of the monomer I_M were plotted as a function of polymer concentration in THF (Figure 2a) and dH_2O (Figure 2b). In both solvents, the I_E/I_M ratios increase with shorter overhang size, a consequence of the smaller drag experienced by the pyrene groups during the process of excimer formation. For all five polymers, the ratios I_E/I_M are consistently smaller in THF than in dH_2O, a consequence of the presence of ground-state pyrene complexes in dH_2O (cf. Figure 1).[9] The ratios I_E/I_M in THF are constant with concentration throughout the polymer concentration range investigated. In water, this behavior is also observed for $EO_{47}PyEO_{87}PyEO_{47}$, $EO_{17}PyEO_{87}PyEO_{17}$, and $EO_{12}PyEO_{87}PyEO_{12}$ but not for $EO_{02}PyEO_{87}PyEO_{02}$ and $PyEO_{87}Py$, for which a clear increase of the I_E/I_M ratios is recorded. These results indicate that excimer is formed intra- and intermolecularly in dH_2O for polymers $EO_{02}PyEO_{87}PyEO_{02}$ and $PyEO_{87}Py$ and intramolecularly *only* in all the other cases.

The steady-state fluorescence measurements were carried out at low polymer concentrations (0.1μM < [Poly] < 2.0 μM), under conditions that were expected to prevent intermolecular associations. Nevertheless intermolecular associations could be probed in dH_2O for the polymers exhibiting the largest hydrophobic character ($EO_{02}PyEO_{87}PyEO_{02}$ and $PyEO_{87}Py$). However it is not the first time that PEG APs have been reported to exhibit intermolecular hydrophobic associations in the micromolar concentration range. Some 34 000 g mol^{-1} linear (telechelic), urethane-coupled poly(ethylene oxide)s with $C_{16}H_{33}O^-$ end groups (HEUR AP) have been reported to form micelles or "rosettes" in dH_2O down to a polymer concentration of 7.4 μM.[18] Although pyrene has a smaller hydrophobic surface than the hexadecanoxy end-groups and a weaker hydrophobic character (a consequence of its smaller molar volume), molecules $EO_{02}PyEO_{87}PyEO_{02}$ and $PyEO_{87}Py$ are still able to associate in dH_2O as HEUR APs do, due to their smaller ethylene oxide content. This illustrates the importance of the balance between hydrophobic and hydrophilic contents.

The hydrophobic intermolecular associations exhibited by $EO_{02}PyEO_{87}PyEO_{02}$ and $PyEO_{87}Py$ in dH_2O have a direct impact on the fluorescence decays of these molecules as can be seen in Figure 3. In dH_2O, the fluorescence decays of $EO_{47}PyEO_{87}PyEO_{47}$, $EO_{17}PyEO_{87}$-$PyEO_{17}$, and $EO_{12}PyEO_{87}PyEO_{12}$ follow a regular trend. As the size of the overhang is shortened, excimer formation is favored by the smaller drag, and the excited pyrene monomer decays faster. This trend is interrupted by $EO_{02}PyEO_{87}PyEO_{02}$ and $PyEO_{87}Py$ which exhibit faster decays at earlier times and slower decays at longer times. These more complicated decays are believed to be an immediate consequence of the intermolecular hydrophobic associations observed with these systems.

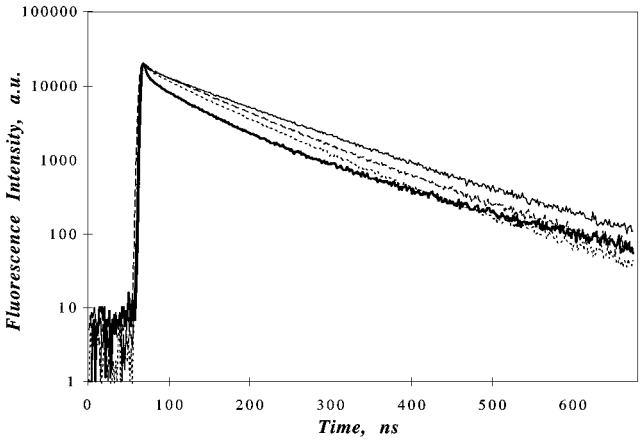

Figure 3. Monomer fluorescence decays ($\lambda_{ex} = 345$ nm; $\lambda_{em} = 376$ nm) of aqueous solutions of (—) EO_{47}—Py—EO_{87}—Py—EO_{47}, (– –) EO_{17}—Py—EO_{87}—Py—EO_{17}, (- - -) EO_{12}—Py—EO_{87}—Py—EO_{12}, and (—) EO_{02}—Py—EO_{87}—Py—EO_{02}. The monomer fluorescence decay of Py—EO_{87}—Py is not shown for clarity reasons.

Intramolecular associations also have a strong effect on the fluorescence decays. Figure 4a shows the monomer and excimer decays of $EO_{47}PyEO_{87}PyEO_{47}$ in THF. The excimer exhibits a 40 ns rise time which results from the encounter delay between an excited and a ground-state pyrene group. The monomer decay is essentially monoexponential (the preexponential weight is 92.3% for a decay time of 153 ns) with a small contribution for a second exponential with a decay time of 40 ns and a preexponential weight of 1.7%. The remaining preexponential weight accounts for the contribution of unquenched pyrene monomer. The monoexponential character of the pyrene monomer decay is expected because the pyrene excimer is known to have a small dissociation rate. These typical characteristics are profoundly altered in Figure 4b, which shows the monomer and excimer decays of the same molecule in dH_2O. The excimer rise time is reduced to 5.5 ns which indicates that some pyrene groups are in close proximity, i.e., preassociated. The monomer decay is essentially monoexponential with a sharp peak at the early times which indicates that excimer formation occurs on a fast time scale, i.e., some pyrene groups are preassociated. These observations agree qualitatively with eqs 4 and 6 which predict that the pyrene monomer should exhibit two very different decay times ($\tau_1 \ll \tau_2$).

For each polymer sample, the monomer and the excimer decays were fitted simultaneously according to eqs 7 and 8 for the monomer and excimer, respectively. The recovered parameters are shown in Table 2. The χ_g^2 values were between 1.00 and 1.77. For polymers $EO_{47}PyEO_{87}PyEO_{47}$ ($\chi_g^2 = 1.00$), $EO_{17}PyEO_{87}PyEO_{17}$ ($\chi_g^2 = 1.14$), and $EO_{12}PyEO_{87}PyEO_{12}$ ($\chi_g^2 = 1.23$), the residuals and autocorrelation functions were randomly distributed around zero. The inadequacy of eqs 7 and 8 to properly fit the fluorescence decays of $EO_{02}PyEO_{87}$-$PyEO_{02}$ ($\chi_g^2 = 1.53$) and $PyEO_{87}Py$ ($\chi_g^2 = 1.77$) is a clear indication that these APs behave in a different manner. An example of the decay fitting is given in Figure 4b.

Degassed solutions of 2-methoxyethyl 4-(1-pyrenyl) butyrate and 4-(1-pyrenyl)butyl methoxytetraethylene glycol 2-ethoxyethyl phosphate give a single exponential decay in water with a lifetime of 140 ns. This lifetime should also be the lifetime of the unquenched pyrene in the PEG samples. However, preliminary triexponential fits of the pyrene monomer decays yield a long lifetime of 170 ns, slightly larger than 140 ns. In our analysis, the lifetime τ_M was fixed at 170 ns. Lengthening of the lifetime of pyrene covalently attached to a water-soluble polymer has already been observed and was attributed to pyrene groups being less accessible to solvent and confined in the polymer coil.[19] Since the pyrene lifetime is only slightly increased (from 140 to 170 ns), the protection offered by the polymer coil has a limited effect.

Discussion

In Table 2, the three polymers with significant overhang all behave in a similar manner. τ_1 is short and the excimer decay exhibits a steep rise-time. The first preexponential weight increases for the monomer and excimer decay indicating an increase in the population of associated ground-state pyrene monomers as the overhang decreases. A lifetime around 55 ± 4 ns is obtained for τ_E which is not unusual for the pyrene excimer.[10] τ_2 decreases with decreasing overhang as would be expected since reduction of the overhang makes internal cyclization easier. The overall pattern however breaks down for the PEGs with no or small (two oxyethylene units) overhang. The χ_g^2 values are definitely larger for these two samples. For polymer Py—EO_{87}—Py, A_{E3} is negative which is physically impossible. The excimer of Py—EO_{87}—Py does not exhibit any rise-time. This indicates that a large population of ground-state aggregates is present in the solution, which supports the steady-state observation that intermolecular association is taking place. Intra- and intermolecular associations for $EO_{02}PyEO_{87}PyEO_{02}$ and $PyEO_{87}Py$ in water demonstrates a more complicated behavior for these polymers than that described by Scheme 1.[21] As a result, only polymers EO_{47}—Py—EO_{87}—Py—EO_{47}, EO_{17}—Py—EO_{87}—Py—EO_{17}, and EO_{12}—Py—EO_{87}—Py—EO_{12} will be analyzed according to Scheme 1.

Kinetic analysis of the parameters listed in Table 2 and carried out according to eqs 4 and 5 yields the rate constants given in Table 3. The rate constants for diffusional encounters $\langle k_D \rangle$ increase with shorter overhang reflecting a smaller drag for internal cyclization. This trend and the magnitude of the $\langle k_D \rangle$ values agrees qualitatively with the $\langle k_D \rangle$ values obtained in organic solvents by Lee and Winnik.[9] For the three polymers, $\langle k_C \rangle$ is much larger than $\langle k_D \rangle$ with $\langle k_C \rangle / \langle k_D \rangle$ being equal to 44 ± 2.

Char et al. estimated experimentally that the *capture* radius equals 20 Å, which is also the hydrodynamic radius of an 87 units PEG chain at room temperature.[20] Although the *capture* volume and the hydrodynamic volume are similar, $\langle k_C \rangle$, which characterizes the chromophores' motion inside the *capture* volume, is 44 times larger than $\langle k_D \rangle$, which represents the chromophores' motion outside the *capture* volume. This large $\langle k_C \rangle / \langle k_D \rangle$ ratio is a reflection on the processes characterizing the motions of the chromophores outside and inside the *capture* volume. Outside the *capture* volume, pyrene groups diffuse randomly. Within the *capture* volume, the pyrene groups are subject to hydrophobic interactions, which generate hydrophobic intramolecular associations. Excimer formation within the capture volume occurs via a local rearrangement of the pyrene groups, which yields the proper pyrene stacking geometry required to form an excimer. It is expected that this process described by $\langle k_C \rangle$ will take place on a faster time

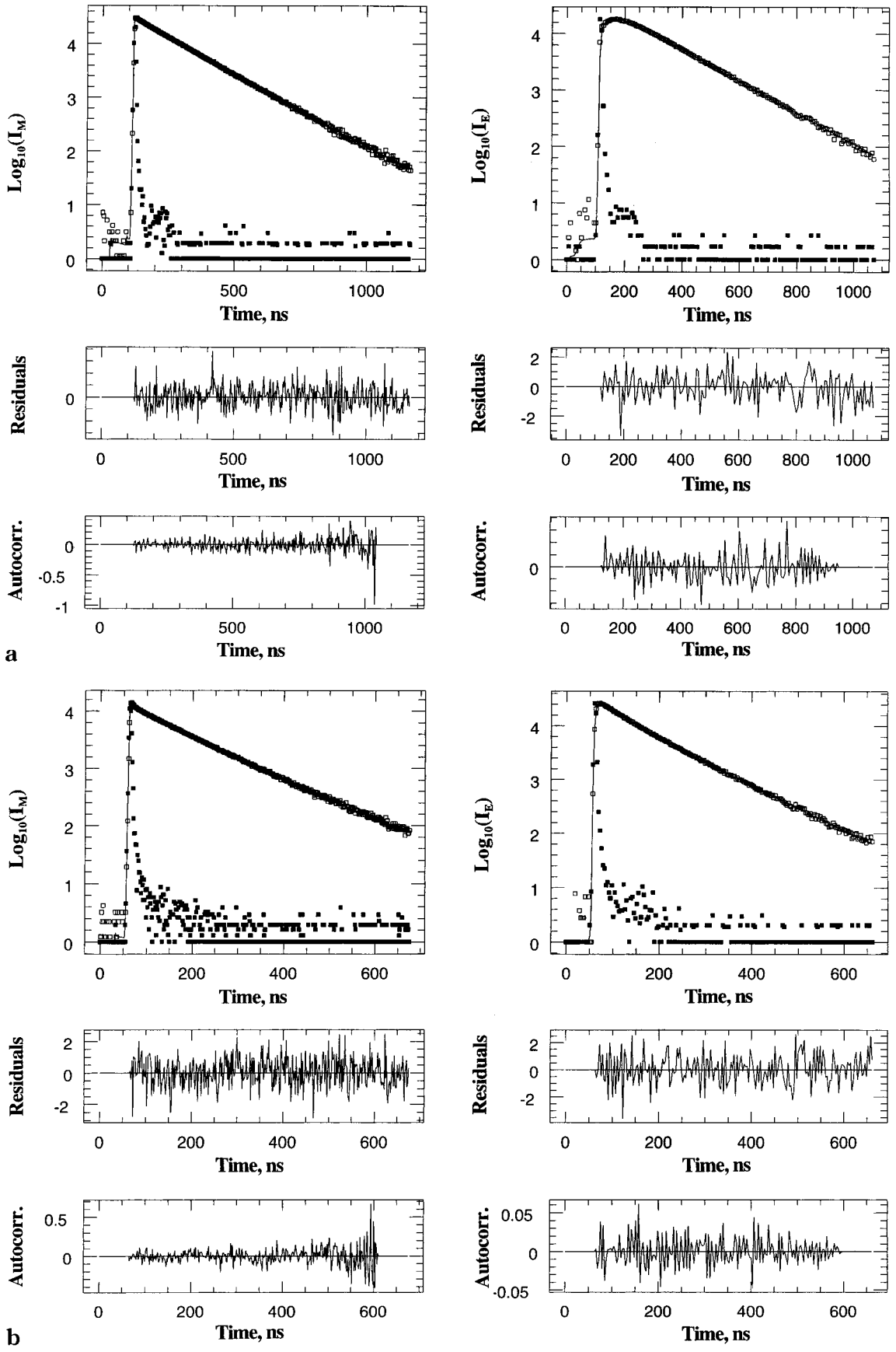

Figure 4. Monomer (λ_{ex} = 345 nm; λ_{em} = 376 nm) and excimer (λ_{ex} = 345 nm; λ_{em} = 510 nm) fluorescence decays of EO_{47}−Py−EO_{87}−Py−EO_{47} in (a) THF and (b) dH_2O. Key: (■) instrumental response function; (□) experimental fluorescence data points, (—) best fit of the fluorescence decay.

Table 2. Fractions of the Preexponential Weights and Lifetimes (τ) Expressed in Nanoseconds Recovered from the Analysis of the Monomer and Excimer Fluorescence Decays of Pyrene Labeled PEGs

sample		exponential 1	exponential 2	exponential 3		χ^2
EO_{47}−Py−EO_{87}−Py−EO_{47}	(M)	0.23 ± 0.01	0.67 ± 0.01	0.10 ± 0.00		
	(E)	−0.41 ± 0.01	1.00 ± 0.00		0.57 ± 0.01	1.00
	(τ)	5.5 ± 0.2	102.3 ± 0.3	170	50.9 ± 1.4	
EO_{17}−Py−EO_{87}−Py−EO_{17}	(M)	0.32 ± 0.01	0.63 ± 0.01	0.06 ± 0.00		
	(E)	−0.50 ± 0.02	1.00 ± 0.00		0.48 ± 0.06	1.14
	(τ)	4.1 ± 0.1	87.2 ± 0.4	170	61.4 ± 2.2	
EO_{12}−Py−EO_{87}−Py−EO_{12}	(M)	0.36 ± 0.01	0.59 ± 0.01	0.04 ± 0.00		
	(E)	−0.52 ± 0.02	1.00 ± 0.00		0.26 ± 0.04	1.23
	(τ)	3.5 ± 0.1	80.6 ± 0.3	170	54.4 ± 3.1	
EO_{02}−Py−EO_{87}−Py−EO_{02}	(M)	0.38	0.51	0.11		
	(E)	−0.47	1.00		0.23	1.53
	(τ)	5.1	64.2	170	66.3	
Py−EO_{87}−Py	(M)	0.22	0.67	0.12		
	(E)	0.24	1.00		−0.65	1.77
	(τ)	19.4	73.1	170	78.1	

Table 3. Kinetic Rates Recovered from the Analysis of the Lifetimes τ_1 and τ_2 (Eqs 4−6)

sample	$\langle k_D \rangle$, 10^6 s^{-1}	$\langle k_C \rangle$, $10^8 s^{-1}$	τ_E, ns
EO_{47}−Py−EO_{87}−Py−EO_{47}	3.9 ± 0.0	1.8 ± 0.1	50.9 ± 1.4
EO_{17}−Py−EO_{87}−Py−EO_{17}	5.6 ± 0.0	2.4 ± 0.1	59.4 ± 2.2
EO_{12}−Py−EO_{87}−Py−EO_{12}	6.6 ± 0.0	2.8 ± 0.1	54.4 ± 3.1

Table 4. Comparison of the Products $\langle k_D \rangle \eta$ Obtained for Pyrene-Labeled PEGs in Water and Organic Solvents

	$\langle k_D \rangle \eta$, kPa			
sample	water[a]	THF[b]	benzene[b]	toluene[b]
EO_{47}−Py−EO_{87}−Py−EO_{47}	3.7 ± 0.0	1.8 ± 0.1	2.2 ± 0.1	2.2 ± 0.1
EO_{17}−Py−EO_{87}−Py−EO_{17}	5.4 ± 0.0	2.1 ± 0.1	2.7 ± 0.2	2.6 ± 0.2
EO_{12}−Py−EO_{87}−Py−EO_{12}	6.3 ± 0.0	2.3 ± 0.2	2.3 ± 0.2	3.6 ± 0.2
EO_{02}−Py−EO_{87}−Py−EO_{02}	n.a.	1.5 ± 0.1	2.2 ± 0.2	2.2 ± 0.2
Py−EO_{87}−Py	n.a.	2.2 ± 0.0	3.0 ± 0.1	3.3 ± 0.2

[a] From this study. [b] From Lee and Winnik (their k_1 values)[9].

Table 5. Contribution of the Different Species at Equilibrium

sample	$f_{[M_D^*]_0}$	$f_{[M_C^*]_0}$	$f_{[E^*]_0}$
EO_{47}−Py−EO_{87}−Py−EO_{47}	0.61 ± 0.01	0.17 ± 0.06	0.22 ± 0.07
EO_{17}−Py−EO_{87}−Py−EO_{17}	0.36 ± 0.03	0.21 ± 0.02	0.43 ± 0.04
EO_{12}−Py−EO_{87}−Py−EO_{12}	0.42 ± 0.05	0.26 ± 0.03	0.33 ± 0.06

scale than the diffusional process described by $\langle k_D \rangle$. Our results indicate that $\langle k_C \rangle$ is 44 times larger than $\langle k_D \rangle$.We find an average $\langle k_C \rangle$ value of $(2.3 \pm 0.5) \times 10^8 s^{-1}$.

It is worth noting that the notion of *capture* volume was also successfully applied toward the quantitative analysis of an ethylene propylene random copolymer grafted with maleic anhydride and labeled with pyrene butanoic acid hydrazide in hexane.[21] In this apolar solvent, polar associations between the maleic anhydride groups induce the formation of pyrene aggregates which form excimer with a $\langle k_C \rangle$ value of $(1.9 \pm 0.3) \times 10^8$ s^{-1}, a value very close to that we obtained for pyrene association in water, a completely different system. $\langle k_C \rangle$ gives the time scale on which associated solvophobic moieties reorganize in a solvent to take their most favored configuration, an information which has biological implications for the folding of hydrophobic residues in proteins.

It is possible to correlate the $\langle k_D \rangle$ values obtained for a same molecule in different solvents by considering the product $\langle k_D \rangle \eta$ where η is the solvent viscosity. This is done in Table 4. Whereas the products $\langle k_D \rangle \eta$ obtained in organic solvents are similar for a given molecule, they are systematically higher in water than in organic solvents (1.7−2.7 times larger). Variations in the $\langle k_D \rangle \eta$ values can be induced by the capture radius and the quality of the solvent. While recognizing the limitations of the detailed meaning of microfluidity and $\langle k_D \rangle$, we will derive an empirical equation which will give a qualitative basis for understanding how various parameters affect these PEG systems. In the bulk, the diffusion rate constant is $k_{diff} = 4\pi N_A R_C D$ where D is the local diffusion coefficient of pyrene and N_A is the Avogadro's number. Within a polymer coil of volume V, one has $\langle k_D \rangle = k_{diff}/N_A V$. For self-diffusion of free pyrene groups in the polymer coil, $D = kT/6\pi\sigma\eta$ where k is the Boltzman constant, T is the absolute temperature, and σ is the reaction radius. The final expression of $\langle k_D \rangle$ is given in eq 9, which will be used on a qualitative basis only.

$$\langle k_D \rangle = \left(\frac{2}{3}kT\right)\frac{1}{\eta}\frac{1}{V}\frac{R_C}{\sigma} \qquad (9)$$

$\langle k_D \rangle$ can be affected by three factors: solvent viscosity, quality of the solvent, and the ratio R_C/σ. A viscous solvent will reduce the rate of pyrene encounter as well as a good solvent which will swell the polymer coil and decrease the local pyrene concentration. The effect of viscosity is taken into account by considering the product $\langle k_D \rangle \eta$. Since water is not a much worse solvent than toluene, benzene and tetrahydrofuran for PEG, the coil volume V does not shrink significantly in water and the enhanced rate of internal cyclization $\langle k_D \rangle$ in water cannot be explained from solvent quality considerations. The other factor that can affect $\langle k_D \rangle$ is the ratio R_C/σ. Char et al. estimated an R_C value of 20 Å for their pyrene end-capped PEG of M_w 4800 in water.[11] Since 7 Å is a good approximation for the reaction radius of pyrene,[22] the ratio R_C/σ could yield a 3-fold increase in the $\langle k_D \rangle$ value in water when compared to that obtained in an organic solvent where R_C equals σ. We conclude from the above that the capture radius certainly contributes to the enhanced $\langle k_D \rangle$ values observed in water.

The preexponential factors in eqs 7 and 8 yield the contributions of all species in the ground state, $f_{[M_D^*]_0}$, $f_{[M_C^*]_0}$, and $f_{[E^*]_0}$. They are given in Table 5. They show that 40−60% of the chains have preassociated pyrene groups.

A previous study showed that a $PyEO_{181}Py$ in water had $\langle k_D \rangle$ and $f_{[M_D^*]_0}$ values of 1.5×10^6 s^{-1} and 0.92, respectively.[5c] A polymer length of 181 ethylene oxide units is equal to that of $EO_{47}PyEO_{87}PyEO_{47}$. The only difference is the position of the pyrene groups which are located at the ends and center for $PyEO_{181}Py$ and EO_{47}-$PyEO_{87}PyEO_{47}$, respectively. $\langle k_D \rangle$ for $PyEO_{181}Py$ is 2.7

times smaller than for $EO_{47}PyEO_{87}PyEO_{47}$. This observation can be qualitatively correlated with the size of the chain spanning the two pyrene groups (N_{Py-Py}) for each molecule. According to eq 9, $\langle k_D \rangle$ is inversely proportional to the coil volume. Assuming that the volume probed by the two pyrene groups (V_{Py-Py}) scales as $(N_{Py-Py})^{3/2}$, we find that V_{Py-Py} is 3.0 times larger for $PyEO_{181}Py$ than for $EO_{47}PyEO_{87}PyEO_{47}$. The structure of the polymer also affects the fraction of unassociated pyrene which is much larger for $PyEO_{181}Py$ ($f_{[M_D^*]_0} = 0.92$) than for $EO_{47}PyEO_{87}PyEO_{47}$ ($f_{[M_D^*]_0} = 0.61$).

Conclusion

In this paper, we have analyzed the complex fluorescence decays of pyrene labeled PEGs in aqueous solutions by deriving a dynamic version of a model initially proposed by Char et al.[11] According to this model, two pyrenes located inside a *capture* volume are attracted to each other, yielding excimer emission. Application of the model to study the monomer and excimer fluorescence decays of a series of pyrene labeled PEGs yielded reasonable kinetic parameters for the PEGs having a significant overhang. When a small overhang or no overhang is present, the model breaks down due to intermolecular aggregation. This finding implies potential differences in the architecture and the kinetics of association between HEUR associative thickeners where the hydrophobic groups are on the chain ends compared with those where the hydrophobic groups are pendant along the chain interior. Inside the *capture* volume, excimers are formed with a very large average rate constant $\langle k_C \rangle$ of $(2.3 \pm 0.5) \times 10^8$ s^{-1} which reflects the hydrophobic interactions that take place between two pyrene groups confined inside the *capture* volume. The diffusion controlled rate constant $\langle k_D \rangle$ indicates that internal cyclization is sensitive to the size of the overhang as observed earlier by Lee and Winnik in organic solvents.[9] However, the $\langle k_D \rangle$ values were found to be much larger (1.7−2.7 times) than expected from simple solvent viscosity considerations. This observation is a consequence of the pyrene groups being brought to the perimeter of the *capture* volume in water, a much larger volume than the *encounter* volume expected in organic solvents. It is the second time that we successfully apply the notion of *capture* volume to account for "complicated" kinetics observed with APs labeled with pyrene.[21]

Finally our model needs three exponentials to fit the monomer and excimer fluorescence decays. These functions are standard functions of commercial software packages for fluorescence decay analysis, a factor which should make this type of analysis easily accessible to the scientific community.

Acknowledgment. J.D. thanks Professor M. A. Winnik for his encouragement to undertake this study. J.D. also thanks NSERC and the University of Waterloo for funding.

References and Notes

(1) Streyer, L. *Biochemistry*, 4th ed.; W. H. Freeman and Co.: New York, 1995; pp 7−11.
(2) Sclavi, B.; Sullivan, M.; Chance, M. R.; Brenowitz, M.; Woodson, S. A. *Science* **1998**, *279*, 1940−1943. Treiber, D. K.; Rook, M. S.; Zarrinkar, P. P.; Williamson, J. R. *Science* **1998**, *279*, 1943−1946. Kellermayer, M. S. Z.; Smith, S. B.; Granzier, H. L.; Bustamante, C. *Science* **1997**, *276*, 1112−1116. Lazardis, T.; Karplus, M. *Science* **1997**, *278*, 1928−1931. Pan, J.; Thirumalai, D.; Woodson, S. A. *J. Mol. Biol.* **1997**, *273*, 7−13. Thirumalai, D.; Woodson, S. A. *Acc. Chem. Res.* **1996**, *29*, 433−439.
(3) Neslon, J. C.; Saven, J. G.; Moore, J. S.; Wolynes, P. G. *Science* **1997**, *277*, 1793−1796.
(4) Schulz, D. N.; Glass, J. E. *Polymers as Rheology Modifiers*; ACS Symposium Series 462; American Chemical Society: Washington, DC, 1989. Glass, J. E. *Polymers Aqueous Media*; Advances in Chemistry Series 223; American Chemical Society. Washington, DC, 1989.
(5) (a) Cheung, S.-T.; Winnik, M. A.; Redpath, A. E. C. *Makromol. Chem.* **1982**, *183*, 1815−1824. (b) Char, K.; Frank, C. W.; Gast, A. P.; Tang, W. T. *Macromolecules* **1987**, *20*, 1833−1838. (c) Duhamel, J.; Yekta, A.; Hu, Y. Z.; Winnik, M. A. *Macromolecules* **1992**, *25*, 7024−7030.
(6) Winnik, M. A. *Acc. Chem. Res.* **1985**, *18*, 73−79.
(7) Winnik, F. M. *Chem. Res.* **1993**, *93*, 587−614 and references herein.
(8) Lee, S.; Winnik, M. A.; Whittal, R. M.; Li, L. *Macromolecules* **1996**, *29*, 3060−3072.
(9) Lee, S.; Winnik, M. A. *Macromolecules* **1997**, *30*, 2633−2641.
(10) Birks, J. B. *Photophysics of Aromatic Molecules*; Wiley & Sons: London, **1970**.
(11) Char, K.; Frank, C. W.; Gast, A. P. *Macromolecules* **1989**, *22*, 3177−3180.
(12) Whittal, R. M.; Li, L.; Lee, S.; Winnik, M. A. *Macromol. Rapid Commun.* **1996**, *17*, 59−64.
(13) Annabale, T.; Buscall, R.; Ettelaie, R.; Whittlestone, D. *J. Rheol.* **1993**, *37*, 695−726.
(14) Demas, J. N. *Excited-State Lifetime Measurements*; Academic Press: New York, 1983.
(15) Boens, N.; Andriessen, R.; Amelot, M.; Van Dommelen, L.; De Schryver, F. C. *J. Phys. Chem.* **1992**, *96*, 6331−6342.
(16) Press: W. H.; Flannery, B. P.; Teukolsky, S. A.; Vetterling, W. T. *Numerical Receipes. The Art of Scientific Computing*; Cambridge University Press: Cambridge, England, 1989.
(17) Duhamel, J.; Yekta, A.; Ni, S.; Khaykin, Y.; Winnik, M. A. *Macromolecules* **1993**, *26*, 6255−6260. Duhamel, J.; Kanyo, J.; Dinter-Gottlieb, G.; Lu, P. *Biochemistry* **1996**, *35*, 16687−16697.
(18) Yekta, A.; Duhamel, J.; Adiwidjaja, H.; Brochard, P.; Winnik, M. A. *Langmuir* **1993**, *9*, 881−883.
(19) Chu, D.-Y.; Thomas, J. K. *Macromolecules* **1984**, *17*, 2142−2147.
(20) Brandrup, J.; Immergut, E. H. *Polymer Handbook*, 3rd ed.; John Wiley & Sons: New York, 1989; Vol. VII, p 22.
(21) Vangani, V.; Duhamel, J.; Nemeth, S.; Jao, T.-C. Submitted for publication in *Macromolecules*.
(22) Duhamel, J.; Winnik, M. A.; Baros, F.; André, J. C.; Martinho, J. M. G. *J. Phys. Chem.* **1992**, *96*, 9805−9810.

MA981160M